Proc. Natl. Acad. Sci. USA
Vol. 90, pp. 11792–11796, December 1993
Neurobiology

Low Ba^{2+} and Ca^{2+} induce a sustained high probability of repolarization openings of L-type Ca^{2+} channels in hippocampal neurons: Physiological implications

OLIVIER THIBAULT, NADA M. PORTER, AND PHILIP W. LANDFIELD*

Department of Pharmacology, University of Kentucky, College of Medicine, MS-305 Chandler Medical Center, Lexington, KY 40536-0084

Communicated by James L. McGaugh, September 13, 1993 (received for review July 30, 1993)

ABSTRACT **Openings of single L-type Ca^{2+} channels following repolarization to negative membrane potentials from a depolarizing step (repolarization openings, ROs) have been described previously in brain cell preparations. However, these ROs have been reported to occur only infrequently. Here we report that the frequency of ROs in cell-attached patches of cultured rat hippocampal neurons can be increased dramatically by lowering the pipette Ba^{2+} concentration to 20 mM from the usual 90–110 mM. This increased opening probability can last for hundreds to thousands of milliseconds following repolarization. Current–voltage analyses of open probability show that the depolarization pulse threshold for inducing ROs in 20 mM Ba^{2+} is −10 to 0 mV but that the probability of ROs reaches maximal levels following depolarizing pulses that approach the apparent null (equilibrium) potential for Ba^{2+}. Comparable current–voltage curves in 110 mM Ba^{2+} from a more positive holding potential (−50 mV) indicate that membrane surface charge screening accounts for some, but not all, of the effect of lowering the Ba^{2+} concentration. Consequently, current-dependent inactivation or some other ion-dependent mechanism (e.g., ion binding inside the pore) also appears to regulate this potentially major pathway of Ca^{2+} entry. A high probability of ROs also can be induced under relatively physiological conditions (5-ms depolarizing steps, 2–5 mM Ca^{2+} in the pipette). Thus, the high open probability state at negative potentials may underlie the long Ca^{2+} tail currents in hippocampus that were described previously and appears to have major implications for physiological functions (e.g., the slow Ca^{2+}-dependent afterhyperpolarization), particularly in brain neurons.**

Multiple types of voltage-activated Ca^{2+} channels have been described in recent years. These differ in pharmacological sensitivity, conductance, voltage dependence, and kinetics and are thought to play varying roles in the regulation of different Ca^{2+}-dependent cellular processes (1–3). Although Ca^{2+} channels deactivate rapidly upon repolarization (4), some Ca^{2+}-dependent processes, such as the slow Ca^{2+}-dependent K^+-mediated afterhyperpolarization (AHP), can last for hundreds to thousands of milliseconds following action potentials (5–7). The long-lasting AHP appears to depend directly on elevated intracellular Ca^{2+} concentration at the membrane (8), but it is unclear how residual intracellular Ca^{2+} from a brief action potential (9) could be sustained for hundreds of milliseconds in the face of rapid Ca^{2+} buffering and diffusion away from the membrane (10, 11).

In recent years, however, there have been several observations consistent with the possibility that Ca^{2+} channel activity may persist following the end of a depolarization. In adult hippocampal slice neurons, very long (> 1 s) whole-cell Ca^{2+} "tail" currents have been observed by use of sharp-electrode voltage-clamp methods. These currents do not appear to be artifactual (12, 13), although whole-cell studies cannot conclusively rule out space clamp errors in process-bearing neurons (14, 15). In addition, several investigators have described single Ca^{2+} channel openings upon repolarization to resting or more negative potentials following a depolarizing pulse (16, 17). Fisher *et al.* (16), studying hippocampal pyramidal neurons, were the first to observe the unusual phenomenon of repolarization openings (ROs) of L-type Ca^{2+} channels at very negative potentials (−70 to −100 mV). These openings could occur up to seconds after repolarization. Similar phenomena have been observed in cultured cerebellar granule cells (17, 18). However, in the previous studies, ROs at resting or more negative potentials were relatively infrequent (16–18).

As in most single Ca^{2+} channel experiments, the previous studies of post-repolarization Ca^{2+} channel openings in brain preparations have used 90–110 mM Ba^{2+} in the pipette as the charge carrier. However, to determine whether ROs might underlie the very long tail-like Ca^{2+} currents in hippocampal neurons (12, 13), we lowered the pipette Ba^{2+} concentration to more closely approximate the extracellular divalent cation concentrations used in whole-cell studies. In the present paper, we report that this procedure strikingly increases the frequency and prolongs activity of L-channel ROs, indicating that, under physiological conditions, ROs may represent a major pathway of Ca^{2+} entry.

MATERIALS AND METHODS

Recording Procedures. Primary cultures of fetal rat hippocampus were established from pregnant Fischer 344 rats (19, 20). Recordings for this study were obtained from a total of 193 patches from hippocampal neurons (22–24°C) according to standard on-cell patch-clamp methods (16, 21) (2- to 5-MΩ pipettes; currents low-pass filtered at 1–2 kHz, digitized at 5–8 kHz). For cell-attached patch recording, the extracellular bath solution used to "zero" the membrane (e.g., ref. 22) was 140 mM potassium gluconate/15 mM NaCl/3 mM $MgCl_2$/10 mM EGTA/10 mM glucose/10 mM potassium Hepes/1 μM tetrodotoxin, pH 7.4. Two main recording pipette solutions were used. The high-Ba^{2+} solution was 110 mM $BaCl_2$/10 mM tetraethylammonium/10 mM Hepes, pH 7.3, whereas the low-Ba^{2+} solution was 20 mM $BaCl_2$/90 choline chloride/10 mM tetraethylammonium/10 mM Hepes, pH 7.3. Recordings also were obtained with pipettes containing 2 or 5 mM $CaCl_2$, 90 mM choline chloride, 10 mM tetraethylammonium, and 10 mM Hepes (pH 7.3). Osmolality of all solutions was adjusted to 320 mOsm with sucrose.

Single-Channel Current Analysis. The total channel open activity ($N \times P_o$) was determined in multichannel patches by integrating the inward current between the leak-subtracted

The publication costs of this article were defrayed in part by page charge payment. This article must therefore be hereby marked "*advertisement*" in accordance with 18 U.S.C. §1734 solely to indicate this fact.

Abbreviations: AHP, afterhyperpolarization; RO, repolarization opening; HP_{RO}, high probability of RO.

*To whom reprint requests should be addressed.

baseline (closed state) to the total open-state current. Average total current, I, was obtained over both the pulse and the post-pulse window and divided by unitary current amplitude, i, at each voltage; total channel open activity was calculated according to the relation $I/i = N \times P_o$, where N is the total number of channels available in the patch and P_o is the probability of a channel being open (22–24). N was estimated from the maximal number of simultaneous L-type channel openings observed in any sweep from that patch (16, 23). For multichannel patches with simultaneous openings at positive voltages, the unitary current, i, was calculated by extrapolating slope conductance from negative voltages with few simultaneous openings. At least four Ca^{2+} channels with significantly different conductances and kinetics (termed T, N, L, and P) have been defined in neuronal preparations (1–3), including hippocampus (16). Except where noted, the dihydropyridine Ca^{2+} channel agonist Bay K 8644 (500 nM) was included in pipette solutions to enhance the contribution of L-type Ca^{2+} channels to total current. Bay K 8644 increases opening frequency and also increases mean open time of L channels from under 1 ms to over 10 ms (16, 23–25); this and the much larger conductance of L-type channels relative to other types indicate that, with Bay K 8644, L channels most likely account for over 95% of total patch current during a pulse above L-channel threshold.

Measures of slope conductance [in current–voltage (I–V) studies] and open times (in protocols similar to Fig. 1) of individual L channels (26) were obtained in smaller patches (one to three channels) with readily identifiable channels and fewer simultaneous openings (26). ROs were defined as openings of Ca^{2+} channels which were closed upon repolarization and then opened. These are different from "true" tail openings, which are already open at repolarization (16). Averaged null traces or hyperpolarizing pulses were used for subtraction of leak and capacitive currents.

RESULTS

Dependence of ROs on Ba^{2+} Concentration. Activity of single Ca^{2+} channels after a depolarizing pulse depends upon the concentration of Ba^{2+} in the cell-attached pipette (Fig. 1). In patches studied with 20 mM Ba^{2+} in the pipette, the frequency of openings after repolarization to −70 mV from a depolarizing step was substantial (Fig. 1*A*). However, in cell-attached patches recorded with 110 mM Ba^{2+} in the pipette, few or no ROs were seen (Fig. 1*B*).

Fig. 1 *C* and *D* show average ensemble currents from patches recorded in 20 and 110 mM Ba^{2+}, respectively. The increase in the frequency of repolarization openings in 20 mM Ba^{2+}, in conjunction with the larger driving force at repolarized levels, can produce a significant and long-lasting ensemble tail current (Fig. 1*C*). In 20 mM Ba^{2+} substantial numbers of ROs can occur for sustained periods (up to seconds) after the depolarizing command step (Fig. 1*E*). Although in some 110 mM Ba^{2+} patches ROs were seen while holding at −70 mV, the ROs occurred in substantially fewer patches in 110 mM Ba^{2+} than in 20 mM Ba^{2+}. The proportion of patches exhibiting at least one clear RO during an I–V analysis from a holding potential of −70 mV was 51/66 patches (77%) in 20 mM Ba^{2+} whereas it was only 14/41 patches (34%) in 110 mM Ba^{2+}. Moreover, in patches that did show ROs, the probability of ROs in 110 mM Ba^{2+} usually was considerably less than in 20 mM Ba^{2+} (see below).

Identification of Channel Types Exhibiting ROs. To verify directly that the ROs we assessed were from L channels, Bay K 8644 was omitted from the pipette in a series of patches (n = 5), and ROs were studied before and after external application of Bay K 8644 (by puffer pipette). In these patches, the mean open time ± SEM of ROs before Bay K 8644 was 2.1 ± 0.22 ms, whereas mean open time of ROs of the same

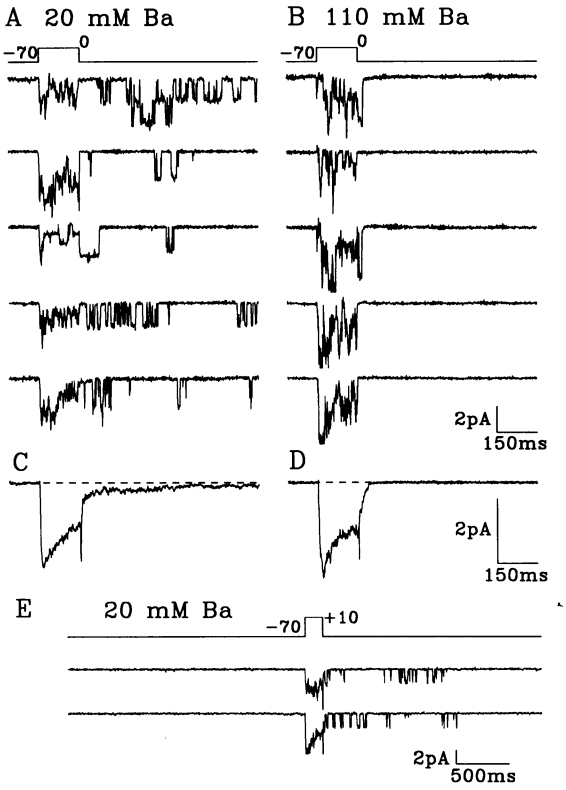

FIG. 1. Effect of Ba^{2+} concentration on ROs. (*A* and *B*) Examples of five traces obtained from five different multichannel patches in 20 or 110 mM Ba^{2+}, selected to be of approximately similar total patch current amplitudes (2–5 pA). Patches were held at −70 mV, depolarized to the command potential of 0 mV for 150 ms, and then repolarized to −70 mV. ROs appeared substantially more frequently with pipette solutions containing 20 mM Ba^{2+} than with 110 mM Ba^{2+}. Recording pipette solutions also contained 500 nM Bay K 8644. (*C* and *D*) Average ensemble current traces obtained in 20 mM and 110 mM Ba^{2+}, respectively, each constructed from 75 sweeps (15 sweeps from each of the five patches). Null traces were included in the analysis. (*E*) Expanded-time examples showing that ROs can occur several seconds after repolarization, and the lack of any spontaneous Ca^{2+} channel activity preceding the pulse.

channels (as identified by the same amplitudes following Bay K 8644) was 13.75 ± 3.5 ms. Each RO of appropriate amplitude to which Bay K 8644 was applied responded with a substantial increase of open time (Fig. 2).

To determine whether ROs represent openings of a different subpopulation of L-type channels and/or whether their gating activity is altered, slope conductances and open dwell times were calculated for channels during the command step (in both 20 and 110 mM Ba^{2+}) and following repolarization (only in 20 mM Ba^{2+} because of the low frequency of ROs in 110 mM Ba^{2+}). Mean conductance values were similar under all three conditions (Figs. 3*A*) and agree well with previously reported conductance values for hippocampal L-type channels (16, 27). Open-time histograms (Fig. 3*B*) were fit with two exponentials (26). However, values for the first time constant (τ_1) were not viewed as accurate in this study due to poor resolution at our filter settings (26) and overlap of N- and T-channel open times with short open times of L channels (16, 22–25). The values we observed for τ_2 of L-type openings in Bay K 8644 (Fig. 3*B*) agree well with previous estimates (22–25). In comparison to values for τ_2 during the depolarizing pulse in either 20 or 110 mM Ba^{2+} (which were not different), the τ_2 for ROs in 20 mM Ba^{2+} was significantly increased. This is consistent with previous observations (16, 18), although the RO-associated open-time prolongation here is superimposed upon a Bay K 8644-induced prolongation.

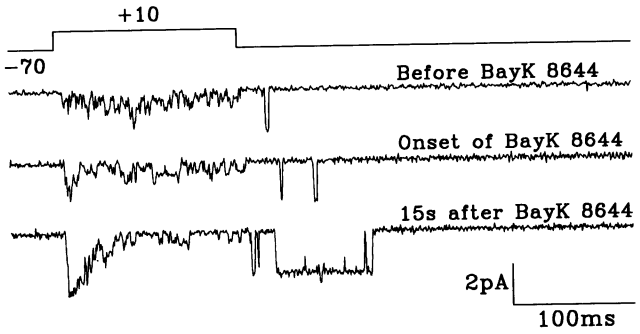

FIG. 2. Dihydropyridine sensitivity of ROs recorded with 20 mM Ba^{2+}, without Bay K 8644 in the recording pipette. Top trace, a single RO is seen following the depolarizing step; middle trace, at the onset of application of Bay K 8644 (100 nM) onto the cell with a puffer pipette, ROs do not yet exhibit dihydropyridine effects, although longer openings during the step are apparent; bottom trace, at 15 sec after the onset of Bay K 8644 application, clear effects of Bay K 8644 on the open time of the amplitude-identified RO can be seen; increased simultaneous channel activity also is seen during the step.

Although the RO analyses here focused primarily on L-type channels, in some patches we observed both brief and longer openings with low amplitude after repolarization. Consequently, further studies will be needed to explore the possibilities that N-channel openings or subconductance openings of L channels (18, 28), or both, also occur following repolarization.

Possible Basis for Suppression of Repolarization Openings by High Ba^{2+}. Several possible mechanisms could account for the large differences between the effects of 110 and 20 mM Ba^{2+} pipette solutions on ROs, including membrane surface charge screening and Ba^{2+} current-dependent inactivation. Charge screening refers to the well-known effect of high concentrations of external divalent cations in shifting the voltage dependence of voltage-activated currents in the positive direction (29). This effect results from reduction of the negative membrane surface potential that arises from fixed anionic groups, through a combination of divalent cation binding to the membrane surface and electrostatic attraction of a layer of divalent counterions (30). This increases the total transmembrane field felt by the channels and therefore requires a greater depolarization for activation. On the other hand, Ca^{2+} current-dependent inactivation of Ca^{2+} channels also is a well-documented phenomenon (31, 32). Moreover, Pitler and Landfield (12) and Kay (33) have observed strong Ca^{2+}-dependent inactivation of Ca^{2+} currents and potentials in hippocampal neurons. In addition, there is evidence that, at least in some systems, including the hippocampus (33), Ba^{2+} current also can induce inactivation of Ca^{2+} channels (34–36).

Preliminary studies of *I–V* curves in 10 patches had indicated that the voltage shift for peak amplitude during the pulse due to charge screening differences was 10–15 mV. To assess the contribution of charge screening to RO probability, the estimated 10- to 15-mV voltage shift from charge screening was more than compensated for by holding patches in 110 mM Ba^{2+} at potentials 20–25 mV more positive than patches in 20 mM Ba^{2+}. From these holding potentials, 10 multichannel patches that showed ROs (5 each at 20 mM and 110 mM Ba^{2+}) were studied in more extensive *I–V* curves (five sweeps at each of 15 command voltages, with each sweep separated by 10 s). Total channel open activity was averaged over the five sweeps for each step and was calculated both during the 150-ms depolarizing command step ($N \times P_{CO}$) and during a 300-ms post-repolarization window ($N \times P_{RO}$). $N \times P_{CO}$ was calculated at steps only to +10 mV (20 mM Ba^{2+}) or +20 mV (110 mM Ba^{2+}) because the small amplitude of channels at steps beyond these voltages made accurate measurement difficult.

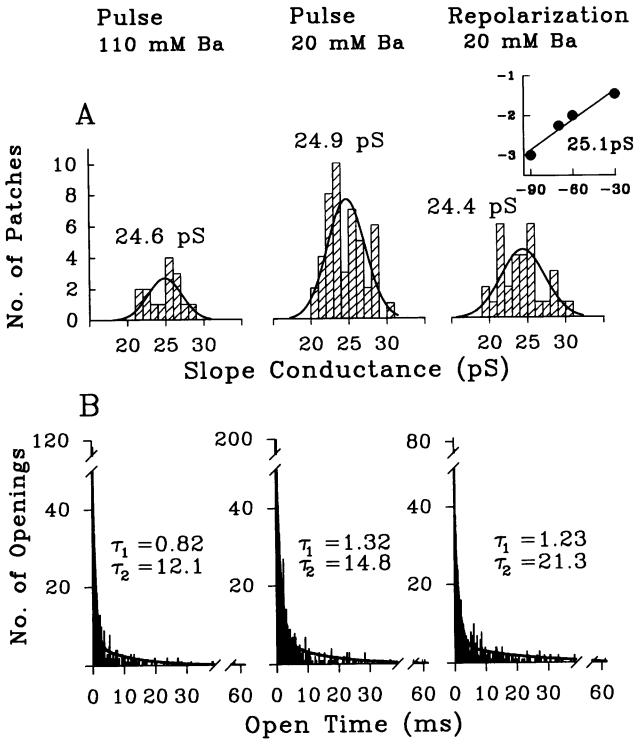

FIG. 3. Single-Ca^{2+}-channel conductance and open dwell times. Ca^{2+} channel amplitudes were measured in patches with one to three channels at different voltage steps during the command potential (110 mM and 20 mM Ba^{2+}) or upon repolarization (20 mM Ba^{2+}). *I–V* plots were calculated for single L-type channels (open time > 1 ms) that could be identified with high likelihood in multiple voltage steps, and slope conductance was calculated by linear regression. ROs were assessed at a more negative voltage range to avoid exceeding the normal activation range of L-type channels. (*A*) Histograms showing the frequency distribution of the single-channel conductances were constructed and fit with Gaussian curves. The mean value for each of the three conditions (in picosiemens) is shown above each of the histogram peaks. The mean single-channel conductances under the three conditions were remarkably close, ranging from 24.4 to 24.9 pS. Data from 15–48 patches were used for each histogram. (*Inset*) Representative single-channel *I–V* plot from ROs at different repolarization voltages. (*B*) Frequency distributions of the open times of single Ca^{2+} channels during the command potential (150-ms duration) in either 110 mM Ba^{2+} or 20 mM Ba^{2+} or upon repolarization (350-ms window) in 20 mM Ba^{2+}. Headings are as in *A*. Histogram bin size was 0.2 ms, with the first two bins excluded from analysis. Histograms were fit with two exponential functions (τ_1 and τ_2).

Fig. 4 shows the *I–V* relationship for multichannel patches studied with either 20 mM or 110 mM Ba^{2+} pipettes and held at −75 mV or −50 mV, respectively. During the step, charge screening in 110 mM Ba^{2+} shifted the voltage dependence of Ca^{2+} channel activity ($N \times P_{CO}$) approximately 14 mV to the right as determined by the shift in half-maximal voltage of the fitted sigmoidal curves. The peak $N \times P_{CO}$ was slightly greater for 20 mM Ba^{2+}, apparently because of a nonsignificant (by Mann–Whitney test) trend to a larger number of channels available in 20 mM Ba^{2+} patches. The mean ± SEM of total channels (N) in the multichannel patches in this experiment was 4.7 ± 0.3 in 20 mM Ba^{2+} (n = 44) and 4.1 ± 0.3 (n = 37) in 110 mM Ba^{2+}.

The threshold for ROs in 20 mM Ba^{2+} occurred following steps to about 0 mV, with $N \times P_{RO}$ rising to maximal levels following steps to voltages in the range +50 to +70 mV. Because of low internal concentrations of divalent cations, Ca^{2+} and Ba^{2+} currents approach reversal potential in a

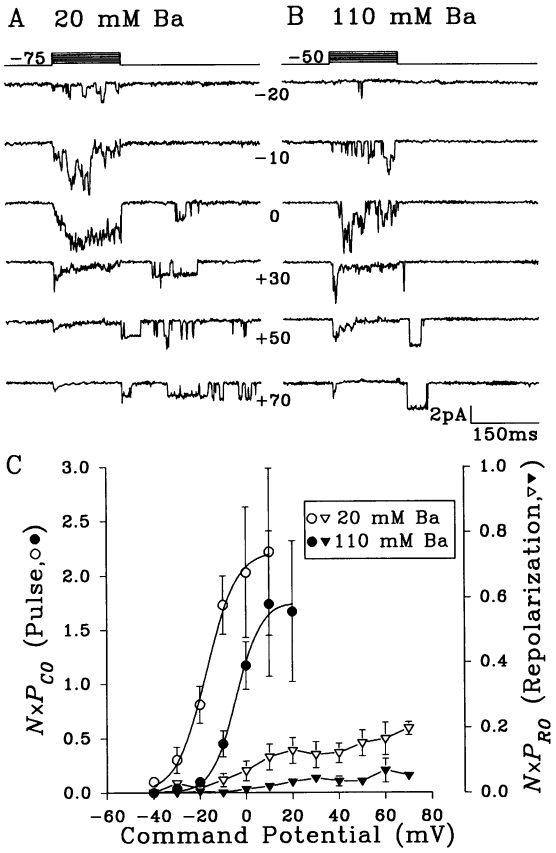

FIG. 4. *I–V* relationships for repolarization and command-step total channel open activity. (*A* and *B*) Representative examples of single-channel traces from *I–V* curves for two cell-attached patches. Holding potential was −75 mV for 20 mM Ba^{2+} and −50 mV for 110 mM Ba^{2+}. (*C*) Plots of the total channel open activity of multichannel patches during the 150-ms command step ($N \times P_{CO}$) and during a 300-ms post-repolarization window ($N \times P_{RO}$) as a function of the voltage step during the *I–V* analysis. The results represent the mean ± SEM ($n = 5$ patches for both $N \times P_{CO}$ and $N \times P_{RO}$ for each Ba^{2+} concentration). In this experiment, the first five patches in each concentration that showed ROs were selected for the extended *I–V* analysis. The activation data points during the pulse ($N \times P_{CO}$) were fit by sigmoidal curves of the form $p(V) = p_{max}/1 + \exp[(V_{1/2} - V)/k]$ (see ref. 16).

nonlinear fashion. However, the +50- to +70-V range appears to approximate the functional null (equilibrium) range for Ba^{2+} current influx (Fig. 4; also see ref. 24). The mean $N \times P_{RO}$ in 110 mM Ba^{2+}, even with repolarization to voltages 25 mV more positive than the holding potential for patches in 20 mM Ba^{2+}, was significantly less than in 20 mM Ba^{2+}. An analysis of variance (two-way, repeated measures) for $N \times P_{RO}$ showed a highly significant effect of Ba^{2+} concentration ($F = 10.97$; $P \leq 0.01$). However, patches in 110 mM Ba^{2+} did exhibit more ROs when repolarized to −50 mV than when repolarized to −70 mV (43% showed at least one RO at −50 mV holding vs. only 34% at −70 mV, and some showed considerable activity at −50 mV).

Relatively Physiological Conditions and ROs. As shown in examples in Fig. 5*A*, ROs also could be induced readily with pipettes containing near-physiological Ca^{2+} concentrations (5 mM). In five patches studied with 5 mM Ca^{2+}, the $N \times P_{RO}$ was 0.17 ± 0.09 for steps from −70 mV to +10 mV, which is generally similar to the range seen in 20 mM Ba^{2+} (Fig. 4*C*). The ROs in 5 mM Ca^{2+} were of much lower amplitude due to the reduced driving force and the lower conductance of Ca^{2+} compared to Ba^{2+} through L-type channels but nevertheless could be clearly resolved. However, ROs appeared to "run down" more rapidly in Ca^{2+} than in Ba^{2+}. In addition, ROs also could be elicited readily with very brief (5-ms) action-potential-like steps to +10 mV (Fig. 5*B*) (also see ref. 17). Similar phenomena occurred in 2 mM Ca^{2+}.

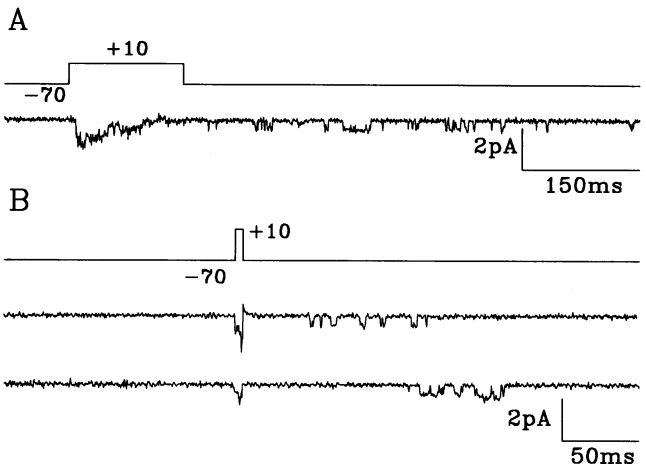

FIG. 5. ROs under relatively physiological conditions. (*A*) Channel activity recorded with a pipette containing 5 mM Ca^{2+} as the charge carrier; openings during the step are poorly resolved, but ROs are clearly seen extending for substantial periods after repolarization. (*B*) Examples of ROs recorded with 5 mM Ca^{2+} in the pipette, in response to 5-ms depolarizing steps to + 10 mV. ROs can be seen following many of the brief depolarizations.

DISCUSSION

The primary observation in this study is that a dramatic increase in the probability of hippocampal L-type channel openings after repolarization can be induced by lowering the external concentration of the divalent cation used as the charge carrier in single-Ca^{2+}-channel recording. This finding clearly implies that ROs can be suppressed by high divalent cation concentrations and, therefore, may yield clues into mechanisms regulating this and other aspects of Ca^{2+} channel activity. Moreover, the time course of the high-probability-of-RO (HP_{RO}) state correlates very closely with that of the AHP and other prolonged Ca^{2+}-mediated processes in brain cells (e.g., very long Ca^{2+} "tail" currents).

The present studies indicate that classical membrane charge screening (29, 30) may play a significant role in the ionic concentration effect but does not seem to account for the entire process. Thus, current-dependent inactivation, or some other ionic suppression process, may play an important role in this phenomenon. The ionic dependence of ROs and the observation that maximal probability of ROs is induced by steps that approach the charge-carrier functional equilibrium potential (Fig. 4), at which point divalent cation influx would be minimal, suggest that the mechanism underlying RO induction by strong depolarization could be the outward displacement of divalent cations from binding sites in the channel pore (37, 38) or from other postulated sites around the channel mouth (37). These sites are important in ion selectivity and permeation but when bound can also block the channel (38). Because the pore sites bind with low affinity (37), they would most likely be sensitive to divalent cation concentration. Alternatively, the mechanism could be related to release from current-dependent inactivation (12, 31–36). There are of course other mechanisms (e.g., conformational changes) through which depolarization might enable ROs, although few can also account for the ionic concentration dependence of ROs. In addition, given the similarity of voltage protocols (strong depolarization) used to induce Ca^{2+} current facilitation or "mode 2" activity in other preparations

(39, 40), it may be that those phenomena reflect related processes that also are regulated in part by ionic concentration.

Other investigators have suggested that ROs depend on voltage-dependent inactivation (17) or a different subtype of L channels characterized by "anomalous gating" (18). However, the ionic dependence and similar conductances (Fig. 3*A*) of ROs suggest that current rather than voltage may regulate ROs and that the same L-channels that do not exhibit ROs in 110 mM Ba^{2+} may be able to do so under different ionic conditions. Nonetheless, the present studies do not preclude the possibility that some subtypes of L channels are unable to generate ROs.

Physiological Relevance of ROs/Tail Currents. Previous studies in this laboratory (12, 13) showed very long whole-cell Ca^{2+} "tail" currents in CA1 cells of adult and aged rat hippocampal slices (with K^+ channels blocked), which appeared to exhibit many of the temporal and voltage dependent properties of the HP_{RO} state reported here. Several investigators have noted that Ca^{2+} channels that open following repolarization might importantly influence a number of Ca^{2+}-dependent processes (e.g., induction of long-term potentiation, enzymatic activation) (16–18). In addition, the results here indicate that post-repolarization Ca^{2+} entry may well be greater than previously recognized and, therefore, could also sustain long-lasting AHPs and other long Ca^{2+}-dependent processes, particularly in brain neurons.

Previous studies have found that the Ca^{2+}-dependent AHP, the Ca^{2+} spike, and whole-cell Ca^{2+} tail-like currents were prolonged and/or larger in hippocampal neurons from aged than from young rats and rabbits (41–43). Thus, alterations in the sustained HP_{RO} state of L-type Ca^{2+} channels might well underlie these aging changes and consequently could modulate aspects of brain aging and, possibly, Ca^{2+}-mediated neuropathologic processes.

We thank Lisa Lowery for excellent assistance with the manuscript, Charles Wash for important technical contributions, and Dr. Alexander Scriabine for the gift of Bay K 8644. This research was supported in part by grants from the National Institute on Aging (AG10836 and AG04542) and Miles.

1. Tsien, R. W., Lipscombe, D., Madison, D. V., Bley, K. R. & Fox, A. P. (1988) *Trends Neurosci.* **11,** 431–437.
2. Miller, R. J. (1987) *Science* **235,** 46–52.
3. Regan, L. J., Sah, D. W. Y. & Bean, B. P. (1991) *Neuron* **6,** 269–280.
4. Swandulla, D. & Armstrong, C. M. (1988) *J. Gen. Physiol.* **92,** 197–218.
5. Hotson, J. R. & Prince, D. A. (1980) *J. Neurophysiol.* **43,** 409–419.
6. Alger, B. E. & Nicoll, R. A. (1980) *Science* **210,** 1122–1124.
7. Barrett, J. N., Magleby, K. L. & Pallotta, B. S. (1982) *J. Physiol. (London)* **331,** 211–230.
8. Eckert, R. & Chad, J. E. (1984) *Prog. Biophys. Mol. Biol.* **44,** 215–267.
9. McCobb, D. P. & Beam, K. G. (1991) *Neuron* **7,** 119–127.
10. Blaustein, M. P. (1988) *Trends Neurosci.* **11,** 438–443.
11. Fryer, M. W. & Zucker, R. S. (1993) *J. Physiol. (London)* **464,** 501–528.
12. Pitler, T. A. & Landfield, P. W. (1987) *Brain Res.* **410,** 147–153.
13. Kerr, D. S., Campbell, L. W., Thibault, O. & Landfield, P. W. (1992) *Proc. Natl. Acad. Sci. USA* **89,** 8527–8531.
14. Johnston, D. & Brown, T. H. (1983) *J. Neurophysiol.* **50,** 464–486.
15. Müller, W. & Lux, H. D. (1993) *J. Neurophysiol.* **69,** 241–247.
16. Fisher, R. E., Gray, R. & Johnston, D. (1990) *J. Neurophysiol.* **64,** 91–104.
17. Slesinger, P. A. & Lansman, J. B. (1991) *Neuron* **7,** 755–762.
18. Forti, L. & Pietrobon, D. (1993) *Neuron* **10,** 437–450.
19. Segal, M. (1983) *J. Neurophysiol.* **50,** 1249–1264.
20. Goslin, K. & Banker, G. (1991) in *Culturing Nerve Cells*, eds. Banker, G. & Goslin, K. (MIT Press, Cambridge, MA), pp. 251–281.
21. Hamill, V. P., Marty, A., Neher, E., Sakmann, B. & Sigworth, F. J. (1981) *Pflügers Arch.* **391,** 85–100.
22. Fox, A. P., Nowycky, M. C. & Tsien, R. W. (1987) *J. Physiol. (London)* **394,** 173–200.
23. Nowycky, M. C., Fox, A. P. & Tsien, R. W. (1985) *Proc. Natl. Acad. Sci. USA* **82,** 2178–2182.
24. Hess, P., Lansman, J. B. & Tsien, R. W. (1984) *Nature (London)* **311,** 538–544.
25. McCarthy, R. T. & TanPiengco, P. E. (1992) *J. Neurosci.* **12,** 2225–2234.
26. Colquhoun, D. & Sigworth, F. J. (1983) in *Single Channel Recording*, eds. Sakmann, B. & Neher, E. (Plenum, New York), pp. 191–264.
27. O'Dell, T. J. & Alger, B. E. (1991) *J. Physiol. (London)* **436,** 739–767.
28. Kunze, D. L. & Ritchie, A. K. (1990) *J. Membr. Biol.* **118,** 171–178.
29. Frankenhauser, B. & Hodgkin, A. L. (1957) *J. Physiol. (London)* **137,** 218–244.
30. Kostyuk, P. G., Mironov, S. L., Doroshenko, P. A. & Ponomaryov, V. N. (1982) *J. Membr. Biol.* **20,** 171–179.
31. Armstrong, D. & Eckert, D. (1987) *Proc. Natl. Acad. Sci. USA* **84,** 2518–2522.
32. Yue, D. T., Backx, P. H. & Imredy, J. P. (1990) *Science* **250,** 1735–1738.
33. Kay, A. B. (1991) *J. Physiol. (London)* **437,** 27–48.
34. Fedulova, S. A., Kostyuk, P. G. & Veselovsky, N. S. (1985) *J. Physiol. (London)* **359,** 431–446.
35. Kasai, H. & Aosaki, T. (1988) *Pflügers Arch.* **411,** 695–697.
36. Mazzanti, M., DeFelice, L. J. & Liu, Y. M. (1991) *J. Physiol.* **443,** 307–334.
37. Kostyuk, P. G., Mironov, S. L. & Shuba, Y. M. (1983) *J. Membr. Biol.* **76,** 83–93.
38. Lansman, J. B., Hess, P. & Tsien, R. W. (1986) *J. Gen. Physiol.* **88,** 321–347.
39. Pietrobon, D. & Hess, P. (1990) *Nature (London)* **346,** 651–655.
40. Artalejo, C. R., Ariano, M. A., Perlman, R. L. & Fox, A. P. (1990) *Nature (London)* **348,** 239–242.
41. Landfield, P. W. & Pitler, T. A. (1984) *Science* **226,** 1089–1092.
42. Moyer, J. R., Thompson, L. T., Black, J. P. & Disterhoft, J. F. (1992) *J. Neurophysiol.* **68,** 2100–2109.
43. Landfield, P. W., Thibault, O., Mazzanti, M. L., Porter, N. M. & Kerr, D. S. (1992) *J. Neurobiol.* **23,** 1247–1260.